

# ChemComm

Accepted Manuscript



This is an *Accepted Manuscript*, which has been through the Royal Society of Chemistry peer review process and has been accepted for publication.

*Accepted Manuscripts* are published online shortly after acceptance, before technical editing, formatting and proof reading. Using this free service, authors can make their results available to the community, in citable form, before we publish the edited article. We will replace this *Accepted Manuscript* with the edited and formatted *Advance Article* as soon as it is available.

You can find more information about *Accepted Manuscripts* in the [Information for Authors](#).

Please note that technical editing may introduce minor changes to the text and/or graphics, which may alter content. The journal's standard [Terms & Conditions](#) and the [Ethical guidelines](#) still apply. In no event shall the Royal Society of Chemistry be held responsible for any errors or omissions in this *Accepted Manuscript* or any consequences arising from the use of any information it contains.

Cite this: DOI: 10.1039/c0xx00000x

www.rsc.org/xxxxxx

ARTICLE TYPE

# Label-free signal-on ATP aptasensor based on the remarkable quenching of tris(2,2'-bipyridine)ruthenium(II) electrochemiluminescence by single-walled carbon nanohorn†

Zhongyuan Liu,<sup>a</sup> Wei Zhang,<sup>a</sup> Wenjing Qi,<sup>a,b</sup> Wenyue Gao,<sup>a,b</sup> Saima Hanif,<sup>a,b</sup> Saqib Muhammad,<sup>a,b</sup> and Guobao Xu<sup>\*a</sup>

Received (in XXX, XXX) Xth XXXXXXXXX 20XX, Accepted Xth XXXXXXXXX 20XX

DOI: 10.1039/b000000x

**The quenching of electrochemiluminescence by single-walled carbon nanohorn has been demonstrated for the first time.**

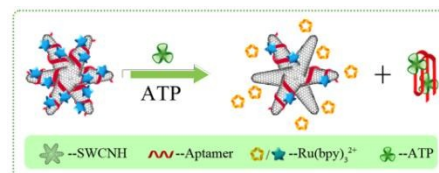
**Moreover, a sensitive, label-free, and signal-on electrochemiluminescence ATP aptasensor is developed using single-walled carbon nanohorn as both quencher and scaffold.**

Electrochemiluminescence (ECL) is chemiluminescence triggered by electrochemical reaction.<sup>1-3</sup> It has now become a very powerful analytical technique for immunoassay, DNA detection, and environmental monitoring, due to its high sensitivity and low background.<sup>4-7</sup> Among many ECL systems, ECL of tris(2,2'-bipyridine)-ruthenium(II) ( $\text{Ru}(\text{bpy})_3^{2+}$ ) with tri-n-propylamine (TPA) as a coreactant has been extensively studied and applied.<sup>8,9</sup> Moreover, the quenching of  $\text{Ru}(\text{bpy})_3^{2+}$  ECL by various quenchers has attracted more and more attentions in recent years,<sup>9-13</sup> because it can be employed as a powerful method for determining specific quencher species or other substances. For example, some ECL biosensors have been developed for small molecules, DNA, and proteins based on the quenching of the  $\text{Ru}(\text{bpy})_3^{2+}$ /TPA ECL by ferrocene and phenol.<sup>13-15</sup> Recently, the quenching of the ECL of the  $\text{Ru}(\text{bpy})_3^{2+}$ /TPA system by carbon nanotube (CNT) has been reported.<sup>8</sup> Meanwhile, a DNA hybridization assay was designed inspired by the above reports using this quenching phenomenon, where single-stranded DNA labeled with  $\text{Ru}(\text{bpy})_3^{2+}$  derivatives probe at the terminus was covalently attached onto the CNT modified electrode.<sup>8</sup> Nevertheless, the quenching of ECL of  $\text{Ru}(\text{bpy})_3^{2+}$  derivatives by nanomaterials has seldom been reported. Label-free and signal-on aptamer-based assays based on the quenching of ECL by CNT have never been reported.

Single-walled carbon nanohorn (SWCNH) has been widely used in various applications, including adsorption, fuel cells, super capacitors, drug delivery, biosensors, and so on.<sup>16-24</sup> It is prepared by  $\text{CO}_2$  laser ablation of pure graphite without using metal catalyst with high yield. In contrast to carbon nanotubes which commonly contain metal impurities, SWCNH is essentially free of metal contamination. It is horn-shaped CNT with a diameter of about 2 to 5 nm and a length of about 50 nm.<sup>25, 26</sup> Typically, SWCNHs assemble to form dahlia-like aggregates with a diameter of about 100 nm (Fig. S1 (ESI<sup>†</sup>)).

Owing to its unique horn-shaped structure, SWCNH has many defects. These defects have strong adsorption capability and may facilitate the quenching by SWCNH. To our knowledge, there are no reports about the quenching of ECL by SWCNH so far.

In this study, the ECL of the  $\text{Ru}(\text{bpy})_3^{2+}$ /TPA system at SWCNH modified glassy carbon electrode (SWCNH/GCE) has been investigated. It is found that the modification of GCE with SWCNH can dramatically quench ECL intensities despite that it can significantly promote the oxidation of TPA and increase the oxidation current of the  $\text{Ru}(\text{bpy})_3^{2+}$ /TPA system. Based on the remarkable quenching effect, a new label-free and signal-on ECL aptasensor is developed using SWCNH as both quencher and scaffold. ATP is selected as a model target. Scheme 1 displays the design concept of the aptasensor. The anti-ATP DNA aptamer is assembled on the SWCNH/GCE by means of a strong  $\pi$ - $\pi$  stacking interaction between nucleobases and SWCNH sidewalls.<sup>23, 27, 28</sup> As a result, more  $\text{Ru}(\text{bpy})_3^{2+}$  molecules may be adsorbed onto the electrode surface via the electrostatic attraction interactions between  $\text{Ru}(\text{bpy})_3^{2+}$  and the negatively charged phosphate backbone of DNA, which shortens the distance between SWCNH and  $\text{Ru}(\text{bpy})_3^{2+}$ , and leads to the effective quenching of ECL. In the presence of ATP, the binding of ATP to aptamer will change the conformation of aptamer, weaken the interaction between SWCNH and  $\text{Ru}(\text{bpy})_3^{2+}$ , and thus inhibit the ECL quenching and increase ECL intensities. Using this label-free and signal-on detection scheme, ATP can be sensitively and conveniently detected by ECL. Since the method does not require any label or amplification, it is simple, time-saving and cost-effective.



**Scheme 1** Schematic illustration of aptamer/SWCNH sensor for ATP detection.

Fig. 1A shows the cyclic voltammogram (CV) of 10.0 mM

TPA obtained at the bare GCE and the SWCNH/GCE in 0.2 M phosphate buffer solutions (pH 7.4). The oxidation current of TPA at the SWCNH/GCE is much larger than that at the bare GCE. In addition, the oxidation peak potential of TPA shifts from ca. +1.0 V at the bare GCE to ca. +0.8 V at the SWCNH/GCE. These results indicate a faster electron transfer rate for the oxidation of TPA at the SWCNH/GCE, which is attributed to the large surface area of SWCNH and plenty of active defects in SWCNH.<sup>16, 29</sup>

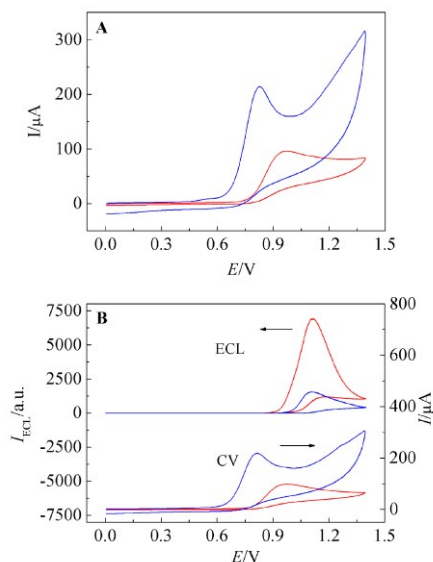
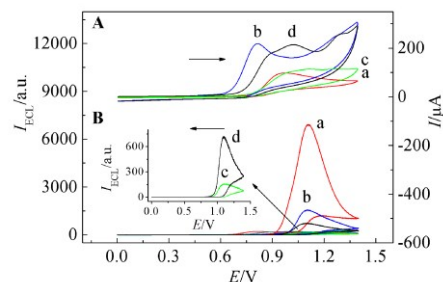


**Fig. 1** (A) CVs of 10.0 mM TPA obtained at the bare GCE (red) and the SWCNH/GCE (blue). (B) CVs and corresponding ECL intensity responses of 1.0  $\mu\text{M}$   $\text{Ru}(\text{bpy})_3^{2+}$  and 10.0 mM TPA obtained at the bare GCE (red) and the SWCNH/GCE (blue). Electrolyte: 0.2 M phosphate buffer solutions (pH 7.4); scan rate: 50  $\text{mVs}^{-1}$ .

CVs and corresponding ECL curves obtained at the bare GCE and the SWCNH/GCE in 0.2 M phosphate buffer solutions containing a low concentration of  $\text{Ru}(\text{bpy})_3^{2+}$  (1.0  $\mu\text{M}$ ) and a high concentration of TPA (10.0 mM) are shown in Fig. 1B. The oxidation current obtained at the SWCNH/GCE (blue) increases about one time compared with that at the bare GCE (red). In contrast, the corresponding ECL intensity decreases about 80% compared with that at the bare GCE. The enhanced oxidation current of TPA at SWCNH is expected to cause enhanced ECL emission, since previous studies show that ECL intensity can be increased through promoting the oxidation of TPA.<sup>29, 30</sup> This remarkable decrease in ECL accompanying with increase in oxidation current demonstrates a strong quenching effect of the SWCNH on the ECL of  $\text{Ru}(\text{bpy})_3^{2+}$ /TPA.

Moreover, the comparison of fluorescence spectra of  $\text{Ru}(\text{bpy})_3^{2+}$  in the absence and presence of SWCNH reveals that SWCNH can quench the fluorescence of  $\text{Ru}(\text{bpy})_3^{2+}$ . As shown in Fig. S2 (ESI<sup>†</sup>),  $\text{Ru}(\text{bpy})_3^{2+}$  exhibits strong fluorescence emission in 0.2 M phosphate buffer solution (red). When 50  $\mu\text{g mL}^{-1}$  SWCNH is added, about 85% of the fluorescence is immediately quenched (blue). The ECL properties of  $\text{Ru}(\text{bpy})_3^{2+}$  may be similar to its fluorescence, because the ECL emission may generate via the same excited state as fluorescence.<sup>4</sup> As already stated, SWCNH is

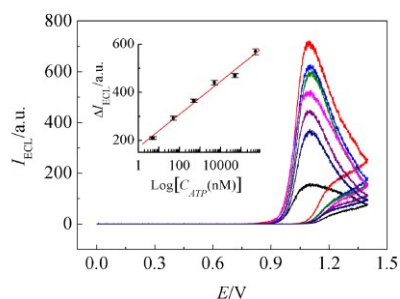
hornshaped CNT.<sup>31</sup> Compared with ordinary multiwall CNT (purity >97%) with a diameter of about 10 to 20 nm and a length of about 5 to 15  $\mu\text{m}$ ,<sup>8</sup> SWCNH quench the ECL of  $\text{Ru}(\text{bpy})_3^{2+}$ /TPA more effectively since 1.0  $\text{mg/mL}$  of SWCNH and 2.0  $\text{mg/mL}$  of CNT have similar quenching effect.



**Fig. 2** CVs and corresponding ECL curves in 0.2 M phosphate buffer solutions (pH 7.4) containing 1.0  $\mu\text{M}$   $\text{Ru}(\text{bpy})_3^{2+}$  and 10.0 mM TPA at a) bare GCE, b) SWCNH/GCE, c) ATP aptamer/SWCNH/GCE, and d) incubated ATP aptamer/SWCNH/GCE with ATP. Scan rate: 50  $\text{mVs}^{-1}$ .

Fig. 2 shows the CVs and corresponding ECL characterization of the different modified procedures of GCE in 0.2 M phosphate buffer solutions (pH 7.4) containing 1.0  $\mu\text{M}$   $\text{Ru}(\text{bpy})_3^{2+}$  and 10.0 mM TPA. The oxidation current at the SWCNH/GCE (Fig. 2Ab) is much larger than that at the bare GCE (Fig. 2Aa) owing to the large surface area and high catalytic activity of SWCNH. The peak current at ATP aptamer/SWCNH/GCE (Fig. 2Ac) is lower than that at SWCNH/GCE (Fig. 2Ab), which indicates that the ATP aptamer is immobilized on SWCNH/GCE successfully via a strong  $\pi$ - $\pi$  interaction between nucleobases and SWCNH sidewalls<sup>23, 27, 28</sup> and reduces the electron-transfer efficiency. The ECL intensity at ATP aptamer/SWCNH/GCE (Fig. 2Bc) is also lower than that at SWCNH/GCE (Fig. 2Bb). The electrostatic attraction interactions between  $\text{Ru}(\text{bpy})_3^{2+}$  and the negatively charged phosphate backbone of the ATP aptamer on ATP aptamer/SWCNH/GCE reduce the distance between the SWCNH and  $\text{Ru}(\text{bpy})_3^{2+}$ , resulting in more effective quenching of ECL. The incubation of ATP aptamer/SWCNH/GCE with ATP changes the structure of ATP aptamer and thus facilitates electron-transfer and greatly increases the redox current (Fig. 2Ad). The ECL intensity also enhances significantly (Fig. 2Bd), because the structural changes of ATP aptamer suppress the ECL quenching.

In order to determine the sensitivity of the prepared ECL ATP aptasensor, the sensor was incubated with different concentrations of ATP. As shown in Fig. 3, the ECL intensities increase with increasing the concentrations of ATP. The ECL enhancement ( $\Delta I_{\text{ECL}}$ ) is proportional to the logarithm of the ATP concentrations ranging from  $5 \times 10^{-9}$  to  $5 \times 10^{-4}$  M with a regression equation  $\Delta I_{\text{ECL}}(\text{a.u.}) = 68.7 \log(C_{\text{ATP}}(\text{nM})) + 171.3$  and a linear correlation of  $R = 0.994$ . The detection limit is 1.0 nM ( $S/N = 3$ ), and the relative standard deviation (RSD) of the sensor for the 1.0  $\mu\text{M}$  ATP is 1.97% ( $n = 3$ ). The present method shows favorable sensing performance as compared to other reported ATP aptasensors

(Table S1 (ESI†)).<sup>32-35</sup>

**Fig. 3** ECL responses for the aptasensor at various ATP concentrations (from bottom to top: 0, 5, 50, 500, 5000, 50000, 500000 nM) in 0.2 M phosphate buffer solutions (pH 7.4) containing 1.0  $\mu\text{M}$   $\text{Ru}(\text{bpy})_3^{2+}$  and 10.0 mM TPA. Inset: calibration curve for the ECL signal increase versus the logarithm of ATP concentrations. The error bars represent the standard deviation of three measurements.

The selectivity of the ATP aptasensor is investigated by comparing the ECL changes induced by three ATP analogues, GTP, CTP, and UTP. As shown in Fig. 4, the ECL changes induced by the analogues above are much smaller than that induced by ATP. It demonstrates that the prepared aptasensor has excellent selectivity for ATP determination due to the inherent specificity of the ATP aptamer toward ATP.

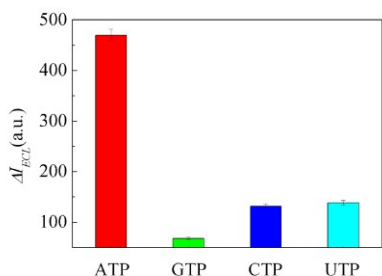


**Fig. 4** ECL signal increase of the aptasensor brought by 50  $\mu\text{M}$  ATP, GTP, CTP, and UTP in 0.2 M phosphate buffer solutions (pH 7.4) containing 1.0  $\mu\text{M}$   $\text{Ru}(\text{bpy})_3^{2+}$  and 10.0 mM TPA. The error bars represent the relative standard deviation of three measurements.

## Conclusions

The efficient quenching the ECL of the  $\text{Ru}(\text{bpy})_3^{2+}$ /TPA system by SWCNH and its application for the development of a label-free, sensitive, and signal-on ECL ATP aptasensor have been demonstrated. Based on the sensitive ECL signal change upon the bind of ATP with ATP aptamer/SWCNH/GCE, the as-fabricated aptasensor shows high sensitivity, wide linear range and good selectivity for ATP. This study shows that SWCNH is a promising ECL quencher, and offers a new avenue for aptamer-based target detection, DNA detection and immunoassays.

## Acknowledgements

This project was supported by the National Natural Science Foundation of China (No. 21475123 & 21175126) and the

Chinese Academy of Sciences (CAS). The authors are very grateful to Professor S. Iijima (Solution Oriented Research for Science and Technology in Japan Science and Technology Agency) for the generous offer of SWCNHs.

<sup>40</sup> <sup>a</sup> State Key Laboratory of Electroanalytical Chemistry, Changchun Institute of Applied Chemistry, Chinese Academy of Sciences, Changchun, Jilin 130022, China. Fax: +86 431 85262747; Tel: +86 431 85262747; E-mail: guobaoxu@ciac.ac.cn

<sup>b</sup> University of the Chinese Academy of Sciences, Chinese Academy of Sciences, No. 19A Yuquanlu, Beijing 100049, PR China.

\*Corresponding author: Prof. G. B. Xu

† Electronic Supplementary Information (ESI) available: Experimental section and supplementary figures. See DOI: 10.1039/b000000x/

1. A. J. Bard, *Electrogenenerated Chemiluminescence*, Marcel Dekker, New York, 2004.
2. M. M. Richter, *Chem. Rev.*, 2004, **104**, 3003-3036.
3. W. J. Miao, *Chem. Rev.*, 2008, **108**, 2506-2553.
4. L. Hu, Z. Bian, H. Li, S. Han, Y. Yuan, L. Gao and G. Xu, *Anal. Chem.*, 2009, **81**, 9807-9811.
5. X.-M. Chen, B.-Y. Su, X.-H. Song, Q.-A. Chen, X. Chen and X.-R. Wang, *TrAC-Trend. Anal. Chem.*, 2011, **30**, 665-676.
6. Y. Xu and E. Wang, *Electrochim. Acta*, 2012, **84**, 62-73.
7. K. Muzyka, *Biosens. Bioelectron.*, 2014, **54**, 393-407.
8. X. Tang, D. Zhao, J. He, F. Li, J. Peng and M. Zhang, *Anal. Chem.*, 2013, **85**, 1711-1718.
9. B. Huang, X. Zhou, Z. Xue and X. Lu, *TrAC-Trend. Anal. Chem.*, 2013, **51**, 107-116.
10. J. McCall, C. Alexander and M. M. Richter, *Anal. Chem.*, 1999, **71**, 2523-2527.
11. J. McCall and M. M. Richter, *Analyst*, 2000, **125**, 545-548.
12. H. Zheng and Y. Zu, *J. Phys. Chem. B*, 2005, **109**, 16047-16051.
13. F. Li, H. Cui and X.-Q. Lin, *Anal. Chim. Acta*, 2002, **471**, 187-194.
14. W. Cao, J. P. Ferrance, J. Demas and J. P. Landers, *J. Am. Chem. Soc.*, 2006, **128**, 7572-7578.
15. L. Chen, Q. Cai, F. Luo, X. Chen, X. Zhu, B. Qiu, Z. Lin and G. Chen, *Chem. Commun.*, 2010, **46**, 7751-7753.
16. X. Liu, H. Li, F. Wang, S. Zhu, Y. Wang and G. Xu, *Biosens. Bioelectron.*, 2010, **25**, 2194-2199.
17. E. Bekyarova, K. Murata, M. Yudasaka, D. Kasuya, S. Iijima, H. Tanaka, H. Kanoh and K. Kaneko, *J. Phys. Chem. B*, 2003, **107**, 4681-4684.
18. D. Tasis, N. Tagmatarchis, V. Georgakilas and M. Prato, *Chem. Eur. J.*, 2003, **9**, 4001-4008.
19. C. M. Yang, Y. J. Kim, M. Endo, H. Kanoh, M. Yudasaka, S. Iijima and K. Kaneko, *J. Am. Chem. Soc.*, 2007, **129**, 20-21.
20. G. Mountrichas, S. Pispas, T. Ichihashi, M. Yudasaka, S. Iijima and N. Tagmatarchis, *Chem. Eur. J.*, 2010, **16**, 5927-5933.
21. J. Miyawaki, M. Yudasaka, T. Azami, Y. Kubo and S. Iijima, *ACS Nano*, 2008, **2**, 213-226.
22. J. Miyawaki, S. Matsumura, R. Yuge, T. Murakami, S. Sato, A. Tomida, T. Tsuruo, T. Ichihashi, T. Fujinmi, H. Irie, K. Tsuchida, S. Iijima, K. Shiba and M. Yudasaka, *ACS Nano*, 2009, **3**, 1399-1406.
23. S. Zhu, Z. Liu, W. Zhang, S. Han, L. Hu and G. Xu, *Chem. Commun.*, 2011, **47**, 6099-6101.
24. S. Zhu, S. Han, L. Zhang, S. Parveen and G. Xu, *Nanoscale*, 2011, **3**, 4589-4592.
25. S. Iijima, M. Yudasaka, R. Yamad, S. Bandow, K. Suenaga, F. Kokai and K. Takahashi, *Chem. Phys. Lett.*, 1999, **309**, 165-170.
26. S. Iijima and T. Ichihashi, *Nature*, 1993, **363**, 603-605.
27. G. Pagona, A. S. D. Sandanayaka, A. Maigne, J. Fan, G. C. Papavassiliou, I. D. Petsalakis, B. R. Steele, M. Yudasaka, S. Iijima, N. Tagmatarchis and O. Ito, *Chem. Eur. J.*, 2007, **13**, 7600-7607.
28. N. Karousis, N. Tagmatarchis and D. Tasis, *Chem. Rev.*, 2010, **110**, 5366-5397.
29. Y. Zu and A. J. Bard, *Anal. Chem.*, 2001, **73**, 3960-3964.
30. Y. Zu and A. J. Bard, *Anal. Chem.*, 2000, **72**, 3223-3232.
31. S. Iijima and T. Ichihashi, *Nature*, 1993, **363**, 603-605.
32. S. Liu, Y. Wang, C. Zhang, Y. Lin and F. Li, *Chem. Commun.*, 2013, **49**, 2335-2337.
33. J. L. Tang, C. Y. Li, Y. F. Li and C. X. Zou, *Chem. Commun.*, 2014, **50**, 15411-15414.

- 
34. Y. J. Liao, Y. C. Shiang, L. Y. Chen, C. L. Hsu, C. C. Huang and H. T. Chang, *Nanotechnology*, 2013, **24**, 444003.
  35. Y. Song, X. Yang, Z. Li, Y. Zhao and A. Fan, *Biosens. Bioelectron.*, 2014, **51**, 232-237.

5